Submarine sand ripples formation in a viscous fluid: 2D and 3D linear stability analysis

V. Langlois[(1)] and A. Valance

(1) Groupe Matière Condensée et Matériaux, UMR 6626, Université Rennes I - 35042 Rennes cedex - FRANCE

Abstract

We investigate analytically the linear stability of a planar sand bed sheared by a laminar boundary layer flow in a 2D and 3D configuration. The sand transport is described by a continuum phenomenological model taking into account the local bed shear stress (calculated from the resolution of the flow over a deformed sand bed), the grain inertia and the local bed slope. We find that the competition between the destabilizing effect of fluid inertia and the stabilizing ones of grain inertia and gravity leads to the selection of a single mode, that is longitudinal (i.e., parallel to the flow direction). The 3D calculation shows that there exists a band of unstable modes in the oblique direction, which can couple to the main longitudinal mode in the non-linear regime to give birth to a two-dimensional pattern no longer invariant in the transverse direction.

1. Introduction

River dunes are structures appearing on river beds made of sand or gravel, *i.e.* under a unidirectional water flow. It means that a granular surface sheared by a continuous flow is unstable and can develop regular patterns. In this paper we investigate the theoretical mechanisms of this instability and derive analytical equations for ripples growth. The first theoretical works on this instability considered potential flows but could not account for the instability without adding artificial phase lags between the flow and the bed profile. Other approaches consisted in solving the turbulent flow over the sand bed. These models are able to predict the ripple instability but the wavelength evaluation of the resulting unstable modes depends greatly on the way how the turbulence is parameterised. Recently, Charru (Charru, 2002) showed that the turbulence is not necessary to get ripple instability. We present here a 2D model, inspired from that of Charru, where the sand transport takes into account both the bed slope effect and the grain inertia one. The later is shown to be the preponderant stabilizing mechanism at high particle Reynolds numbers and to determine the most dangerous wavelength. We also extend the model to the 3D configuration, and show that oblique modes are unstable and can couple to the most unstable longitudinal mode in the non-linear regime. As a result, we expect that at the first stage of the instability, a pattern invariant in the transverse direction first emerges and then evolves towards a “brick” pattern.

2. 2D model equations

We consider a Newtonian and viscous fluid flowing over a deformed sand bed. Outside the boundary layer this flow is assumed to be unidirectional and uniform. The dimensions of the bed deformation are supposed to be small compared to those of the laminar boundary layer.

The main assumption is the quasi-stationarity: the flow is calculated as if the bed were fixed. This means that the flow adapts itself instantaneously to a change of the bed profile. This allows us to solve the stationary hydrodynamic equations. Within this approximation the flow equations are given by:

$$r\,(\mathbf{u}\cdot\mathbf{grad})\,\mathbf{u} = -\mathbf{grad}\,p + h\,\Delta\mathbf{u} \qquad (1)$$

$$\text{div}\,\mathbf{u} = 0 \tag{2}$$

and are associated to the following boundary conditions :

$$\mathbf{u}(h) = \mathbf{0} \quad \text{on the sand bed surface} \tag{3}$$

$$\mathbf{u}(L) = U_\infty \mathbf{e_x} \quad \text{at the top of the boundary layer} \tag{4}$$

where h is the height of the bed profile, L the thickness of the boundary layer and U_∞ is the flow velocity outside the boundary layer.

The basic state of the flow corresponds to the situation where the sand bed surface remains flat and horizontal. In that case, the flow velocity profile is given by a simple linear profile:

$$U_0(z) = \frac{U_\infty z}{L} = g\ z \tag{5}$$

where γ is the shear rate.

The sand bed is described as a continuum. The equilibrium flux of transported grains in a fully developed state is given by the Meyer-Peter law (Fredsøe, 1992):

$$q^{eq} \propto \left(\Theta - \Theta_c\right)^{3/2} \tag{6}$$

where Θ is the Shields parameter defined as $\Theta = t\ /\ r\,(s-1)gd$ (τ is the shear stress at the sand bed, s the relative density of the sand in comparison with that of the fluid, d the sand grain diameter and r the density of the fluid). Θ_c is the critical Shields number above which grains start to move. The critical Shields parameter is found to depend on the local slope of the bed as follows:

$$\Theta_c = \Theta_{c_0}\left(1 + \frac{1}{\tan f_s}\frac{\partial h}{\partial x}\right) \tag{7}$$

where f_s is the internal angle of friction and Θ_{c_0} is a numerical constant corresponding to the critical Shields number for an horizontal flat sand bed.

A model based on the division of the grains into two separate populations (respectively static and moving grains), inspired from the BCRE model of granular avalanches (Bouchaud, 1995), is used to account for the inertia of grains (Valance, 2003). This analysis leads to the expression of the actual flux of grains:

$$\frac{\partial q}{\partial x} = -\frac{q - q_{eq}}{l_{eq}} \tag{8}$$

l_{eq} stands for the characteristic length necessary for a grain to reach the equilibrium with the flow, starting from an out-of-equilibrium situation. It depends on the drag force exerted by the fluid on the grain and in the linear approximation $l_{eq} = f(\text{Re}_p)\,d\,s$ where f is a function of the particle Reynolds number Re_p wich is constant for high values of Re_p and scales as Re_p for low ones.

The closure of this formulation is given by the mass conservation of sand grains:

$$\frac{\partial h}{\partial t} = -\frac{\partial q}{\partial x} \tag{9}$$

The analysis consists in calculating the evolution of a perturbation of the bed of the form:

$$h(x, z, t) = h_1(z)\, e^{\mathrm{i}\, k_x x + w t} \tag{10}$$

where h_1 is a small quantity. Note that the wave number k_x characterises the spacing of the crests, the imaginary part of ω/k_x represents the phase velocity of the perturbation whereas the real part of w corresponds to its growth rate. It is important to note that equation (9) implies that a perturbation grows only if the imaginary part of the transport rate q is negative, that is, in particular, if there is a phase lag between the grain flux and the bed profile.

3. Two-dimensional analysis

We first calculate the flow perturbation over a one-dimensional bed. The calculation strategy employed is the same as that exposed in (Vittor, 1992) and (Charru, 2000). We will focus here on the situation where the height L of the boundary layer is much larger than the characteristic length scales of the sand bed deformation. This calculation leads to an analytical expression of the perturbed Shields number calculated at the sand bed to first order in h_1:

$$\Theta_1 \propto \frac{\mathrm{Ai}(-ie^{ip/6} b^{4/3})}{\int_0^\infty e^{-?} \mathrm{Ai}(x')\mathrm{d}x} \tag{11}$$

where Ai is the first Airy function, $b = k l_n = k\sqrt{n/g}$ is the dimensionless viscous length, and $x' = e^{ip/6}(x - ib^2)/b^{2/3}$.

Then linearizing the equations governing the sediment transport and the bed height, we get a close equation for the growth rate of the bed perturbation:

$$w \propto m\, \Theta_{c_0}^{3/2}\, m^{1/2} \left[-i \frac{\Theta_1}{\Theta_{c_0}} \frac{k}{h_1} - \frac{k^2}{\tan f_s} \right] \frac{1 - ikl_{\mathrm{eq}}}{1 + k^2 l_{\mathrm{eq}}^2} \tag{12}$$

where $m = (\Theta_0 - \Theta_{c_0})/\Theta_{c_0}$. The parameter m measures the distance from the threshold of grain motion and will be referred to as the relative shear stress excess.

If we neglect the effects of the gravity (*i.e.*, $f_s = p/2$) and of grain inertia (*i.e.*, $l_{\mathrm{eq}} = 0$), the real part of the growth rate ω of the perturbation is given on (Fig. 1). We conclude that the bed is unstable against any perturbation, and the shortest wavelengths are the most unstable. However, according to the experimental observations, one particular mode should be selected. That is why we need to introduce stabilizing mechanisms like gravity and grain inertia. We will first include the gravity effect in the sediment transport. Second, we will take into account grain inertia effect, neglecting bed slope effect. At last, we will treat the general situation where both effects are included.

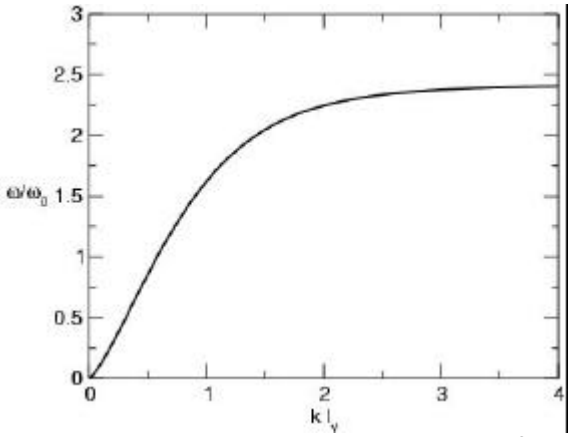

Fig. 1 – Growth rate for small values of β

3.1 Gravity regime

Setting $l_{eq} = 0$ in equation (12), the growth rate becomes, in the long wavelength limit ($b << 1$) :

$$w \propto 0.53(1+m)\, b^{4/3} - \frac{b^2}{\tan f_s} \tag{13}$$

The selection of a particular mode results from the competition between the destabilizing mechanism of the fluid flow, proportional to $k^{4/3}$, and the stabilizing one due to bed slope effect, proportional to k^2. The order of magnitude of the fastest growing mode is then given by the balance of these two terms. One gets :

$$l_{\max} = \frac{30 l_n}{(\tan f_s)^{3/2}(1+m)^{3/2}} \tag{14}$$

The evolution of $l_{\max}$ as a function of μ is shown on (Fig. 2). In the case of sand grains in water flow, we obtain $l_{\max} = 0.5\,\text{cm}$ for grains of diameter $d = 50\,m\text{m}$ and shear stress excess $m = 1$, which seems to be underestimated in comparison to the available experimental data.

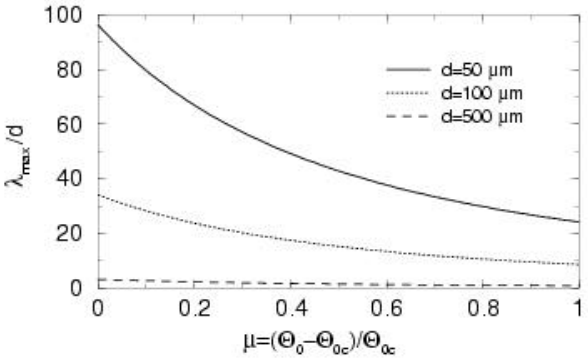

Fig. 2 – Most unstable wavelength vs. relative shear stress excess (grain inertia neglected).

3.2 Inertia regime

We neglect here the effect of the bed slope on the sediment transport but take the grain inertia into account, which is expected to be pertinent when Re_p is larger than one. In this case, the growth rate reads in the long wavelength limit:

$$w \propto 0.53\, b^{4/3} - 0.9\, \frac{l_{eq}}{l_n}\, b^{7/3} \tag{15}$$

The grain inertia also plays a stabilizing role for short waves and scales as $k^{7/3}$. The most unstable mode is then given by:

$$l_{max} = 19\, f(Re_p)\, \frac{r_g}{r}\, d \tag{16}$$

and its evolution as a function of the relative shear stress excess is shown on Fig.3. In the case of sand grains in water flow and shear rate corresponding to high particle Reynolds number, we obtain $l_{max} = 9.5\,\mathrm{cm}$ for grains of diameter $d = 500\,\mu\mathrm{m}$, which seems to be in better agreement with experiments.

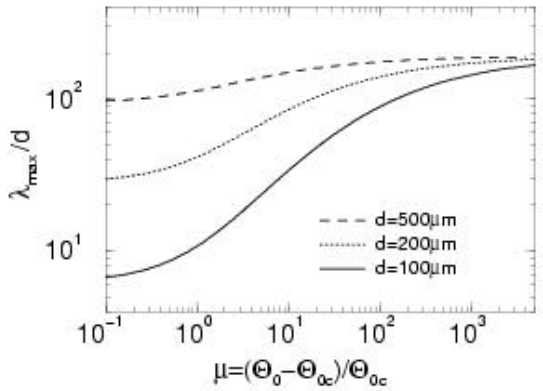

Fig. 3 – Most unstable wavelength vs. relative shear stress excess (gravity neglected).

3.3 General case

At last, we analyze the general situation where both stabilizing effects are taken into account.

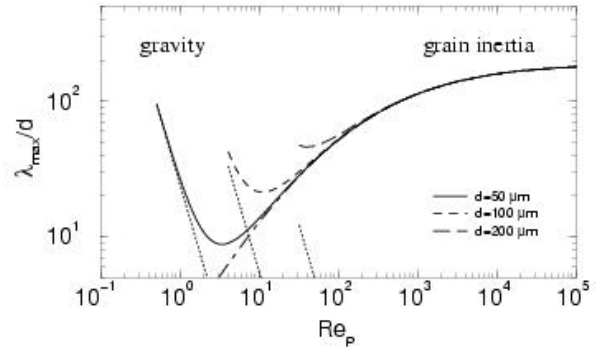

Fig. 3 – Most unstable wavelength vs. particle Reynolds number

The transition between the gravitational and inertial regimes occurs at a critical particle Reynolds number Re_{pc} which is found to depend on the grain diameter (see on Fig. 3), or more precisely on the Galileo number (Valance, 2003). As an example, we obtain, in a water flow, $\mathrm{Re}_{p_c} \approx 2$ for grain diameter of $50 mm$ and $\mathrm{Re}_{p_c} \approx 80$ for grain diameter of $500 mm$. As a conclusion, the most dangerous mode is driven by gravity for small particle Reynolds numbers and by inertia for larges ones. There exists a cross-over regime at intermediate values of Re_p.

4. 3D Analysis

4.1 Extension of the model in 3D

We now extend the previous analysis to the three dimensional configuration, i.e., a unidirectional flow over a two-dimensional deformed bed of the form:

$$h(x, y, z, t) = h_1(z) e^{\mathrm{i}(k_x x + k_y y) + w t} \tag{17}$$

Equations (1-2) with boundary conditions (3-4) can also be analytically solved in the 3D case and the shear stress at the sand surface can be again expressed in terms of integrals of Airy functions (Langlois, 2003).
The expression for the equilibrium flux of transported grains can be extended to the 3D situation. On the base of the analysis of Fredsoe et al (Fredsoe, 1992), one can derive the following 3D law for the transport rate:

$$\mathbf{q} = (\Theta - \Theta_c)^{3/2} \left(\frac{(\Theta_x + n_z n_x)\mathbf{e}_x + (\Theta_y + n_z n_y)\mathbf{e}_y}{\sqrt{(\Theta_x + n_x n_z)^2 + (\Theta_y + n_y n_z)^2}} \right) \tag{18}$$

where $\mathbf{n} = (n_x, n_y, n_z)$ is the unit vector normal to the sand surface. We recall that $Q = (\Theta_x, \Theta_y, \Theta_z)$ is the dimensionless shear stress evaluated at the sand surface. The critical Shields number is found to depend on the local slope of the bed surface as follows:

$$\Theta_c = \Theta_{c_0} \left(1 + \frac{1}{\tan f_s} (\mathbf{e}_z - n_z \mathbf{n}) . \frac{Q}{\Theta} \right) \tag{19}$$

Finally, the mass conservation in the 3D configuration reads

$$\frac{\partial h}{\partial t} = -\mathrm{div}\, \mathbf{q} \tag{20}$$

For simplicity, we will neglect here the inertial effects so that $\mathbf{q} = \mathbf{q_{eq}}$. The inertial effects can also be included in a 3D model, but this will not be exposed in this paper.

4.2 Results

Using the same strategy as that exposed in 2D, we can derive an analytical expression for the growth rate of a perturbation of mode $\mathbf{k}$:

$$w \propto \Theta_{c_0}^{3/2} m^{1/2} \left[-i \frac{\Theta_{1x}}{\Theta_{c_0}} \frac{k_x}{h_1} - \frac{k_x^2}{\tan f_s} \right] + \frac{\Theta_{c_0}^{1/2} m^{3/2}}{1+m} \left[-i \frac{\Theta_{1y}}{\Theta_{c_0}} \frac{k_y}{h_1} - \frac{k_y^2}{\tan f_s} \right] \quad (21)$$

where Θ_{1x} and Θ_{1y} are the x and y component of the perturbed dimensionless shear stress and can be expressed in terms of integrals of Airy functions (Langlois, 2003). From the dispersion relation, one can plot the stability diagram (see Fig. 5). The left panel in Fig. 5 corresponds to the case where the stabilizing effect of gravity is neglected. In that case, arbitrarily infinite large longitudinal wave number k_x are unstable, as in the 2D situation. The novelty in comparison to the 2D case is the presence of unstable oblique modes (with $k_y \neq 0$). Taking into account gravity effect (right panel in Fig. 5), one gets a band of unstable modes of finite width in the longitudinal and transverse direction. The fastest growing mode is found to be on the horizontal axis: it means that the most dangerous mode is a longitudinal mode (see Fig. 6 where the growth rate is plotted as a function of the wave numbers k_x and k_y). As a consequence, in the first stage of the instability the sand bed will develop a ripple pattern invariant along the y direction. However, in the non-linear regime one can expect that the unstable oblique modes will couple with the main longitudinal mode and gives birth to a 2D pattern where the invariance along the y direction disappears.

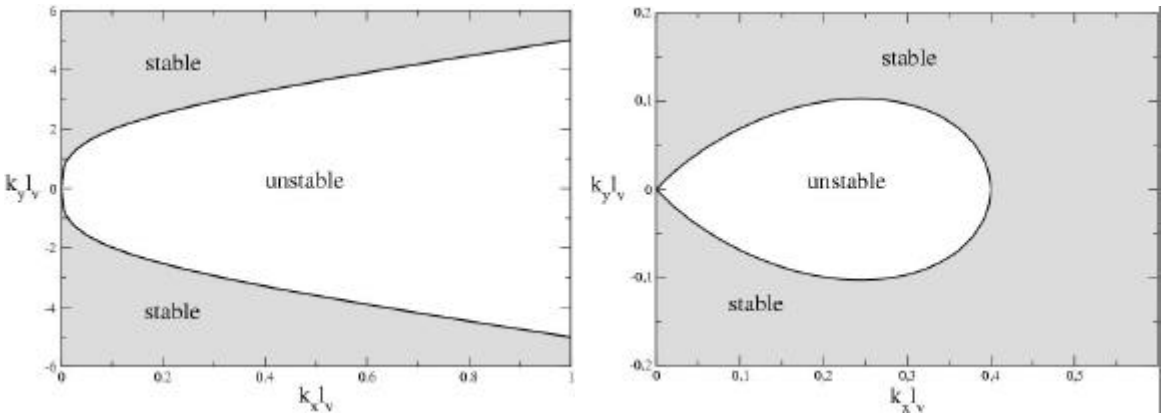

Fig. 5 – Stability diagram.
(left: without gravitational effect; right: with the gravitational effect).

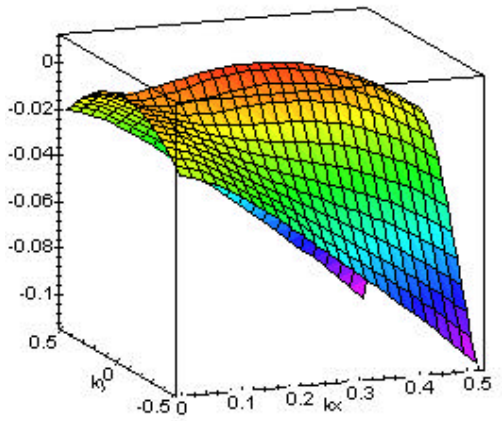

Fig. 6 – Growth rate for long wavelengths

5. Conclusion and Perspectives

We presented in this paper a linear stability analysis of a sand surface submitted to a viscous fluid shear in 2D and 3D configuration. The sand transport was described by a continuum model taking into account the local bed shear stress (calculated from the resolution of the flow over a deformed bed), the grain inertia and the bed slope. We found that the selected mode (or equivalently the most unstable mode) results from the balance of the destabilizing effect of the fluid inertia and the stabilizing ones of gravity and grain inertia. In 2D as well as in 3D, the most unstable mode is longitudinal, resulting in the development of a sand pattern invariant along the transverse direction. The specificity in 3D is the presence of unstable oblique modes whose dynamics are dominated by the main longitudinal mode in the linear regime. However they are expected to couple with the main longitudinal mode in the non-linear regime and give birth to 2D "brick" pattern. This last result should be checked by a non-linear analysis.

References

J.-P. Bouchaud et al., *Phys. Rev. Lett.*, Vol. 74, 1995.

F. Charru and H. Mouilleron-Arnould, Instability of a bed of particles sheared by a viscous flow, *J. Fluid Mech.*, Vol. 452, pp. 303-323, 2002.

F. Charru and J. Hinch, J. Fluid Mech., Vol. 414, pp. 195-223, 2000.

J. Fredsøe and R. Deigaard, *Mechanics of coastal sediment transport*, World Scientific, 1992.

V. Langlois and A. Valance, *preprint*, 2003.

A. Valance and V. Langlois, Formation of ripples over a sand bed. Part I, submitted to *Phys. Rev. E*

A. Valance, Formation of ripples over a sand bed. Part II, submitted to *Phys. Rev. E,* 2003.

G. Vittori and P. Blondeaux, Sand ripples under sea waves. Part 3, *J. Fluid Mech.*, Vol. 239, pp. 23-45, 1992.